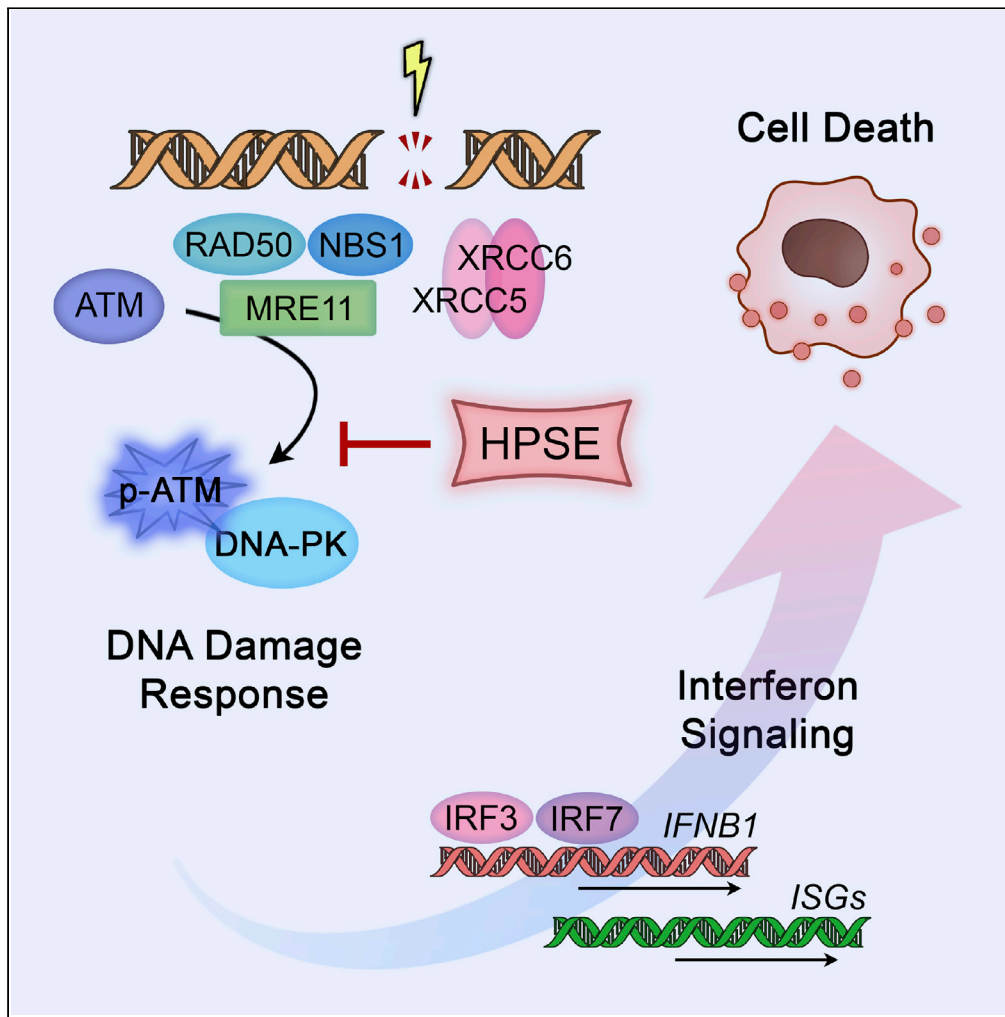


Article

Dissociation of DNA damage sensing by endoglycosidase HPSE



Alex Agelidis,
Rahul K.
Suryawanshi,
Anaamika
Campeau, David
J. Gonzalez,
Deepak Shukla

dshukla@uic.edu

HIGHLIGHTS

HPSE binds key proteins at interface of DNA damage signaling and IFN responses

Nuclear translocation of DNA damage transducer ATM is enhanced in absence of HPSE

Cells lacking HPSE display enhanced sensitivity to DNA damage-induced death

HPSE interfaces with regulators of DNA damage response to influence cell fate



Article

Dissociation of DNA damage sensing by endoglycosidase HPSE

Alex Agelidis,^{1,2} Rahul K. Suryawanshi,² Chandrashekhar D. Patil,² Anaamika Campeau,^{3,4} David J. Gonzalez,^{3,4} and Deepak Shukla^{1,2,5,*}

SUMMARY

Balance between cell proliferation and elimination is critical in handling threats both exogenous and of internal dysfunction. Recent work has implicated a conserved but poorly understood endoglycosidase heparanase (HPSE) in the restriction of innate defense responses, yet biochemical mediators of these key functions remained unclear. Here, an unbiased immunopurification proteomics strategy is employed to identify and rank uncharacterized interactions between HPSE and mediators of canonical signaling pathways linking cell cycle and stress responses. We demonstrate with models of genotoxic stress including herpes simplex virus infection and chemotherapeutic treatment that HPSE dampens innate responses to double-stranded DNA breakage by interfering with signal transduction between initial sensors and downstream mediators. Given the long-standing recognition of HPSE in driving late-stage inflammatory disease exemplified by tissue destruction and cancer metastasis, modulation of this protein with control over the DNA damage response imparts a unique strategy in the development of unconventional multivalent therapy.

INTRODUCTION

Although discovered decades ago as a key extracellular component serving as an attachment point for numerous growth factors, cellular signals, and microbes, the glycosaminoglycan heparan sulfate (HS) continues to be assigned new functions in the maintenance of cellular homeostasis and regulation of disease (Aquino et al., 2010; Xu and Esko, 2014; Zhang et al., 2014). Despite its prevalence across cell types and the existence of many situational structural modifications, our understanding of this sugar molecule and its regulatory enzymes is far from complete. One such enzyme, heparanase (HPSE), is known to be the only mammalian protein capable of splitting chains of HS into smaller subunits (Rabelink et al., 2017). Through its action on cell surface and intracellular HS, HPSE is now known to contribute to disease processes including inflammation, destruction of tissue architecture, and metastasis (Hong et al., 2012; Kundu et al., 2016; Vlodavsky et al., 2018, 2020). More recent work has demonstrated an important contribution of HPSE to microbial pathogenesis, particularly through the promotion of viral egress and the cultivation of an inflammatory milieu conducive to viral spread. Initial studies in this realm were performed in herpes simplex virus 1 (HSV-1), and multiple investigations proved similar actions of this protein across viral families including dengue virus, hepatitis C virus, adenovirus, and human papillomavirus (Agelidis and Shukla, 2020; Agelidis et al., 2017; Guo et al., 2017; Hadigal et al., 2015; Puerta-Guardo et al., 2016; Thakkar et al., 2017). As a prototypic DNA virus that uses HS for initial cellular attachment, HSV-1 has been used as a model cellular perturbation to study the various roles of HPSE in driving pathogenesis. HSV-1 most commonly causes vesicular mucocutaneous eruptions of the oral or genital areas; however, these can progress to more serious sequelae in some individuals, such as encephalitis, vertical transmission to neonates, or ocular keratitis. Our poor grasp of why certain individuals progress to these more serious consequences, along with the fact that all clinical trials of vaccines directed against viral components have failed, points to the importance of a more comprehensive understanding of host factors in driving infection (Belshe et al., 2012; Stanberry et al., 2002). In studying this widespread pathogen that has infected a majority of the global population, investigators now understand that the virus' ability to evade host defense responses has played a large part in its genetic success (Chan and Gack, 2016; Orzalli and Knipe, 2014). Evasion of the DNA damage response is one such mechanism. HSV-1 and other viruses have established through their natural drive to propagate over ages of evolution (Christensen and Paludan, 2017). Likewise, dampening of natural

¹Department of Microbiology and Immunology, University of Illinois at Chicago, Chicago, IL 60612, USA

²Department of Ophthalmology and Visual Sciences, University of Illinois at Chicago, Chicago, IL 60612, USA

³Department of Pharmacology, University of California, San Diego, La Jolla, CA 92093, USA

⁴Skaggs School of Pharmacy, University of California, San Diego, La Jolla, CA 92093, USA

⁵Lead contact

*Correspondence: dshukla@uic.edu

<https://doi.org/10.1016/j.isci.2021.102242>



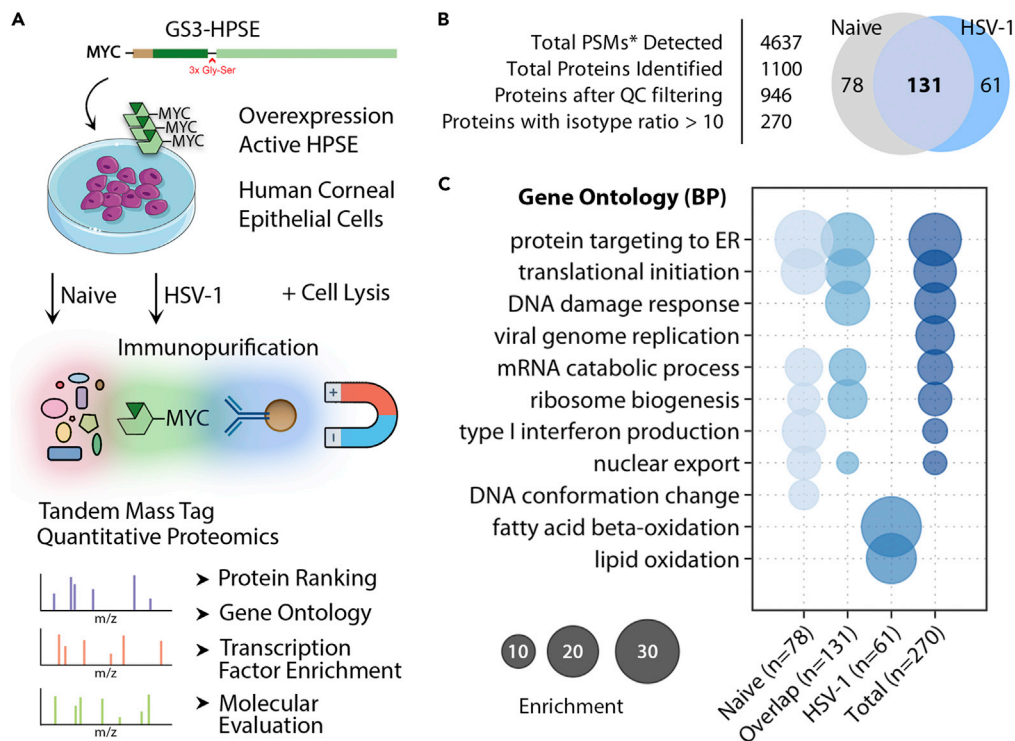


Figure 1. Immunopurification-mass spectrometry (IP-MS) analysis ties HPSE to a dense network of proteins regulating cell cycle and stress responses

(A) Schematic of IP-MS procedure for the quantification of proteins bound to HPSE in human corneal epithelial (HCE) cells in the presence and absence of HSV-1 infection.

(B) Left: numbers of peptides identified by quantitative proteomics analysis fitting specified criteria. Right: Venn diagram of proteins with immunopurification to isotype ratio >10. *PSMs, peptide spectrum matches.

(C) Gene ontology (biological process) analysis performed on each portion of the Venn diagram described in (B).

antiviral immune responses including production of type I interferons allows viral replication to proceed undetected. Interestingly, a number of recent publications have described robust associations between these two pathways: cellular sensing of DNA damage can cause robust induction of type I interferon; however, the molecular mechanisms that connect these systems remain to be characterized (Dunphy et al., 2018; Hartlova et al., 2015; Yu et al., 2015). Here we demonstrate that HPSE serves as an important intermediary between DNA damage and interferon production, an intersection with extensive implications in the development of human disease.

RESULTS

Interaction between HPSE and multiple proteins in cell cycle regulation and biogenesis

Given a dearth of biochemical evidence in the literature to explain our recent finding that HPSE acts as a potent regulator of cellular stress responses (Agelidis et al., 2021), we undertook a quantitative proteomics analysis of immunopurified HPSE to investigate the molecular interactions involved (Figure 1A). Isolation of myc-tagged HPSE from human corneal epithelial cells and subsequent immunopurification-mass spectrometry (IP-MS) analysis yielded 270 proteins with a ratio of >10 versus isotype antibody pull-down, indicating that HPSE has the capacity for interaction with many more cytoplasmic and nuclear proteins than previously known (Figures 1B and S1). "GS3" signifies the coding sequence for the fully proteolytically processed form of HPSE that was used in this assay. The HPSE protein sequence was also predicted by NucPred to contain two nuclear localization sequences that may contribute to its previously documented ability to enter the nucleus under various circumstances and interact with nucleic acids (Figure S1) (Brameier et al., 2007; Rivara et al., 2016). Gene Ontology and overlap analysis of these HPSE-binding proteins shows robust enrichments of various metabolic functions required for cellular proliferation, including "translational initiation," "ribosome biogenesis," and "mRNA catabolic process" (Figure 1C). Individual

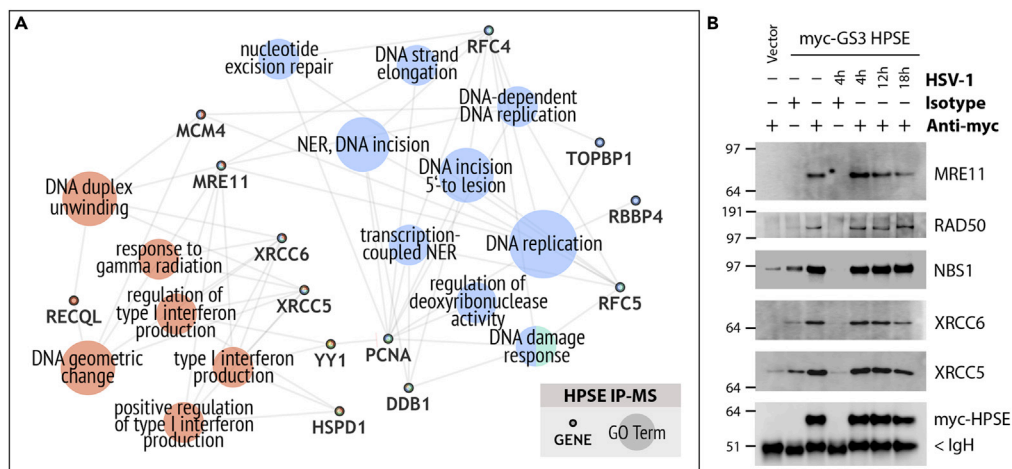


Figure 2. HPSE binds multiple key proteins at the interface of DNA damage signaling and interferon response
(A) Proteins and corresponding Gene Ontology terms overrepresented in HPSE IP-MS. Network analysis performed with ClueGO in Cytoscape.
(B) Western blot confirmatory analysis of myc-HPSE immunopurified from human corneal epithelial (HCE) cells and probed for binding to multiple sensors of double-stranded DNA breaks. Isotype indicates non-specific mouse IgG of the same immunoglobulin subtype as anti-myc IP antibody.

consideration of each portion of the Venn diagram generated a notion of which processes may be active in the presence or absence of HSV-1 infection. Further promoter motif analysis using the PASTAA algorithm indicates that binding partners of HPSE are likely regulated by several major transcription factors, including CREB1 and the related ATF1, ATF2, and ELK1, known for their roles in driving cell proliferation; E2F1, a key cell cycle regulator; and STAT1, which is heavily implicated in the production and response to type I interferon (Figure S2) (Bommareddy et al., 2018; Ivashkiv and Donlin, 2014; Mayr and Montminy, 2001; Roeder et al., 2009). Support for the impact of these transcription factors with respect to HPSE actions also comes from our recent work showing that HPSE restricts multiple innate stress responses (Agelidis et al., 2021). This unique analysis thus draws an initial indirect connection between HPSE and multiple important drivers of cellular proliferation and defense.

HPSE binds multiple key proteins at the interface of DNA damage signaling and interferon response

Considering these newly identified HPSE interactions in conjunction with similar enrichments by an alternative STRING-based method drove us to investigate the possibility that HPSE integrates signals between the pathways of type I interferon generation and response to DNA damage (Figure 2A). Interestingly, multiple recent studies have demonstrated that innate immune responses including production of type I interferons are activated upon cellular sensing of DNA damage, yet the precise biochemical mediators of these connections remain unknown (Dunphy et al., 2018; Hartlova et al., 2015; Yu et al., 2015). In our hands, repeat immunopurifications of HPSE in human cells showed robust binding of MRE11, RAD50, NBS1, XRCC5, and XRCC6, proteins heavily implicated in DNA damage sensing and repair (Figure 2B). These sensors are known to bind particularly to regions of double-stranded DNA breaks and have been recently established as important drivers of type I interferon production and signaling (Dunphy et al., 2018; Hartlova et al., 2015; Yu et al., 2015). The association of HPSE with the DNA damage response thus appears specific to the apparatus of double-stranded DNA breaks as no interactions with proteins involved in nucleotide excision, base excision, or single-stranded DNA breaks were identified by the IP-MS approach.

Nuclear preclusion of double-stranded DNA damage transducer ATM by HPSE upon genotoxic stress

Upon further analysis of the parallel HPSE-deficient mouse embryonic fibroblast (MEF) system, it became clear that cells respond more robustly to DNA damage in the absence of HPSE. Nuclear localization of phosphorylated ataxia telangiectasia mutated (p-ATM) and total cellular phosphorylated ATM substrates (noted by the specific p-S*/T*Q motif) were used as markers of activation of the DNA damage sensing system

(Traven and Heierhorst, 2005). Likewise, HSV-1 and etoposide, a chemotherapeutic known for its ability to induce dsDNA breaks through the inhibition of topoisomerases, were used as inducers of DNA damage in cells containing and lacking HPSE. Phospho-ATM expression and nuclear localization and subsequent phosphorylation of ATM substrates are markedly increased in cells deficient in HPSE after induction of a DNA damage stimulus, whether through etoposide or viral infection (Figure 3A). Image analysis of multiple thresholded confocal micrographs using CellProfiler on an individual cell basis yielded highly significant increases in activation of the ATM system in the absence of HPSE (Figures 3B–3D). Etoposide was also found to preferentially induce IFN- β in the absence of HPSE, further supporting the notion that HPSE serves as an important link between DNA damage and IFN signaling (Figure 3E). Transcription of the downstream interferon stimulated gene 15 (ISG15) is dramatically elevated in HPSE-deficient cells, and is unchanged by HSV-1 or etoposide, suggesting that the interferon system is constitutively active in the absence of HPSE (Figure 3F).

HPSE interfaces with regulators of DNA damage response to influence cell fate

Large increases in cell death were also noted in cells without HPSE upon exposure to etoposide, based on propidium iodide uptake from culture media in cells with loss of membrane integrity (Figures 4A and 4B). Treatment with KU-55933, a specific commercial inhibitor of DNA damage sensor ATM, shows that this enhanced sensitivity to DNA damage is mediated through ATM in HPSE-deficient cells (Figures 4B and 4C). Propidium iodide index indicates the quotient of propidium iodide-stained events to Hoechst (cell-permeable nucleic acid stain)-positive events. Although etoposide was found to be a more effective driver of cell death than HSV-1 infection, treatment of HPSE-deficient cells with KU-55933 successfully prevented the induction of cell death in both cases (Figure 4C). Further investigation into the biochemical mediators of the DNA damage response in HPSE-deficient cells confirmed that ATM phosphorylation is elevated in the absence of HPSE (Figure 4D). Initial phosphorylation of ATM precedes phosphorylation of the downstream mediator checkpoint kinase 2 (CHK2) and phosphorylation of the histone H2Ax at serine 139 to produce γ H2Ax, all indicators of activation of the DNA damage response. Western blot analysis of the ATM substrate motif p-S*/T*Q also indicates a differential pattern of downstream activation that remains to be explored. In the case of HSV-1 infection, which is a multifactorial set of processes involving a multitude of cellular factors in addition to DNA damage, this phosphorylation of ATM appears later in the time course (Figure 4E). Phosphorylated CHK2 was not detected in this system, although differential phosphorylation of γ H2Ax was still apparent.

With an additional focus on the mechanism of etoposide-induced cell death occurring in the absence of HPSE, we observed that apoptosis is promoted at later time points. Drivers of apoptosis including caspase-3 and caspase-8 are cleaved after etoposide treatment of HPSE-deficient cells, whereas this is not observed in wild-type cells under these treatment conditions. On the other hand, cleavage of caspase-1 and gasdermin D, classically associated with activation of pyroptosis, is not seen. Collectively, these results suggest that HPSE acts to suppress ATM activation, potentially by serving as an insulator of signaling from the MRE11-RAD50-NBS1 complex to downstream mediators of the DNA damage response including CHK2.

Inhibitor modulation of cell death induced by etoposide

Chemical inhibitors of various forms of cell death and the DNA damage response were used to further dissect the involvement of HPSE in these processes induced by etoposide (Figures 5A–5C). Representative immunofluorescence images of cells treated in the presence of the dyes CellEvent Caspase-3/7 green reagent and propidium iodide indicate the extent of apoptosis and loss of membrane integrity, respectively. Nec-1, an inhibitor of RIPK1 and necroptosis, and belnacasan, an inhibitor of caspase-1, showed no effect on apoptosis and loss of membrane integrity compared with vehicle treatment. ZVAD, a potent inhibitor of all caspases, showed a marked decrease in apoptosis activation and some degree of reduction in propidium iodide cellular influx. KU-55933 (ATMi) treatment does display initial rescue of apoptosis until the final collection time, where prolonged cellular toxicity of this compound likely dominates. Interestingly, treatment with mirin, a chemical inhibitor of the MRN complex, protects cells from etoposide-induced apoptosis and eventual loss of membrane integrity, and exhibits a similar profile to ZVAD in these assays. Together these findings suggest again that HPSE plays an important role as a regulator of DNA damage response signals acting through the MRN complex.

DISCUSSION

With this exploration of various cellular responses to genotoxic stress, we demonstrate that HPSE serves as a key intersection between the detection and effector phases of signal transduction in the regulation of cell

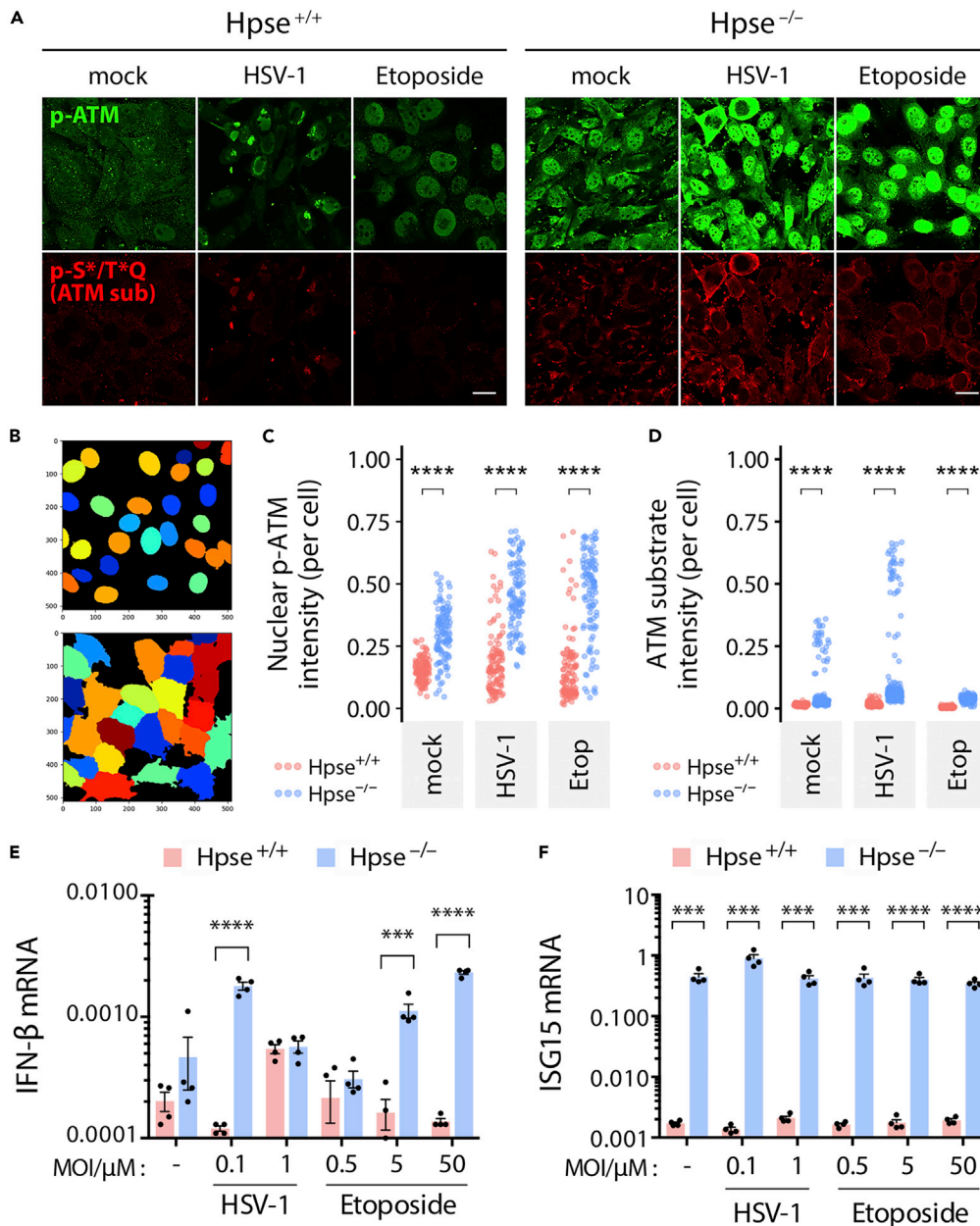


Figure 3. Nuclear preclusion of DNA damage response transducer ATM by HPSE upon genotoxic stress

(A) Representative immunofluorescence micrographs displaying extent of phosphorylated ATM (green) and ATM substrate phosphorylation motif (p-S*/T*Q) (red) 8 h after exposure to HSV-1 (MOI = 1) or etoposide (50 μM) in Hpse^{+/+} and Hpse^{-/-} MEFs. Scale bar, 20 μm.

(B) Demonstration of thresholding method performed with CellProfiler to quantify nuclear and total fluorescence intensity of individual cells.

(C and D) Quantification of fluorescence intensity of p-ATM present in individual nuclei (C) or ATM substrates present in whole cells (D). Significance determined by Wilcoxon signed-ranks test.

(E and F) Quantitative PCR measurement of IFN-β (E) and ISG15 (F) transcripts relative to β-actin after treatment of wild-type and HPSE-deficient MEFs with indicated agents at specific MOIs/concentrations for 24 h (HSV-1) or 8 h (etoposide). Data are represented as mean ± SEM. Significance determined by Mann-Whitney test (n = 4). ***p < 0.001, ****p < 0.0001.

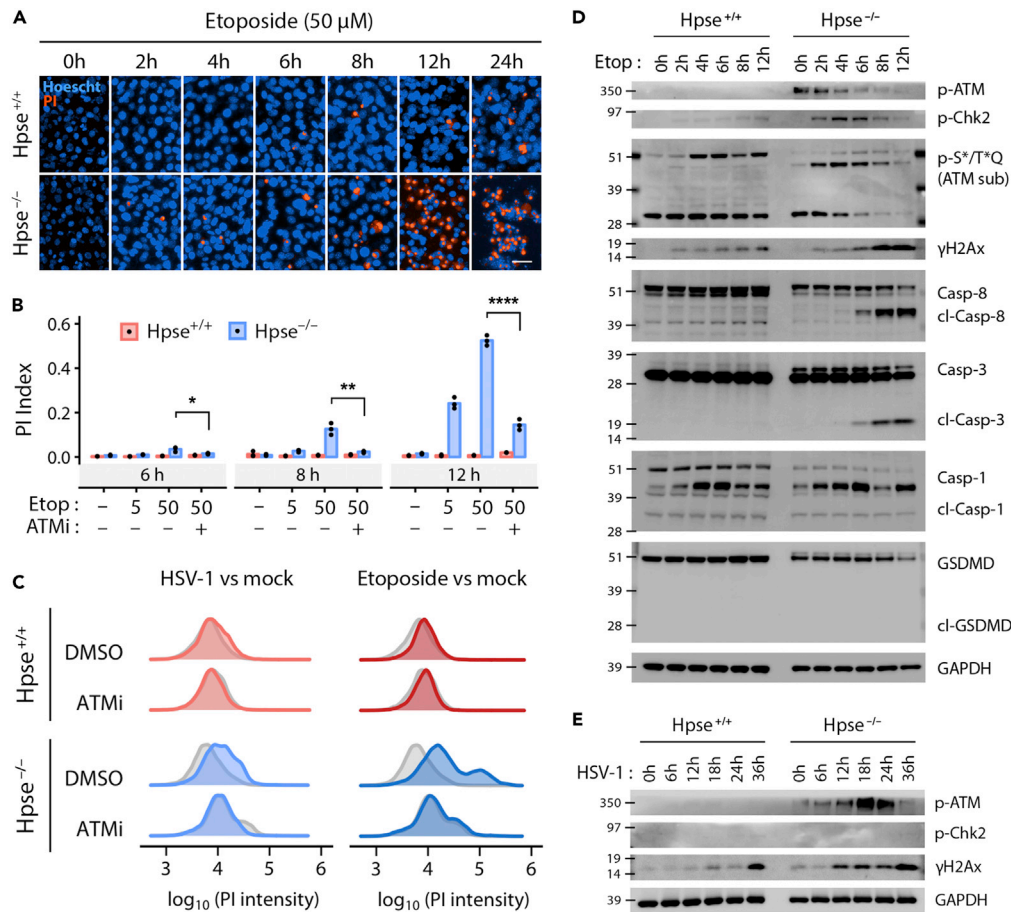


Figure 4. HPSE interfaces with regulators of DNA damage response to influence cell fate

(A) Cell death upon induction of dsDNA breaks with etoposide, measured by uptake of propidium iodide (PI) stain from culture medium in Hpse^{+/+} and Hpse^{-/-} MEFs. Hoechst nucleic acid stain is permeable to all cells, whereas PI only fluoresces upon loss of membrane integrity. Scale bar, 50 μ m.

(B) Quantification of cell death in Hpse^{+/+} and Hpse^{-/-} MEFs with varying doses of etoposide and ATM kinase inhibitor (ATMi, KU-55933 10 μ M) at indicated times post treatment. Data are represented as mean \pm SEM. Significance determined by Mann-Whitney test (n = 3).

(C) Representative flow cytometry analysis of PI uptake of cells pre-treated for 18 h with DMSO vehicle or ATMi 10 μ M, followed by either HSV-1 for 24 h (left) or etoposide for 8 h (right). Mock (gray) curves denote cells that were pre-treated and then received no further stressor.

(D) Representative western blot analysis of Hpse^{+/+} and Hpse^{-/-} MEFs treated with etoposide at 50 μ M for specified times.

(E) Representative western blot analysis of Hpse^{+/+} and Hpse^{-/-} MEFs infected with HSV-1 KOS at MOI = 0.1 for specified times.

*p < 0.05, **p < 0.01, ****p < 0.0001.

cycle and DNA damage responses. HPSE non-enzymatic activity in particular has been implicated in an array of cellular pathways, yet the mechanism of these roles remains unclear (Coombe and Gandhi, 2019; Jayatilleke and Hulett, 2020). Our recent study established that HPSE displays an inhibitory role over type I interferon and downstream responses (Agelidis et al., 2021). Based on results of the current work, HPSE non-enzymatic binding of proteins involved in DNA damage response, particularly MRE11, RAD50, and NBS1, is likely key in the dampening of interferon responses observed in our studies. Model agents of DNA damage used in this study were etoposide and HSV-1 KOS, which is a strain commonly used by laboratories studying HSV-1 infection worldwide. Other more virulent strains, including McKrae and 17, are likely to be more effective at inducing DNA damage, the details of which will be analyzed in future studies. At multiple doses of etoposide and with a low MOI of 0.1, cells without HPSE are more sensitive to induction of IFN- β transcription. One explanation for the lack of significant difference in IFN- β

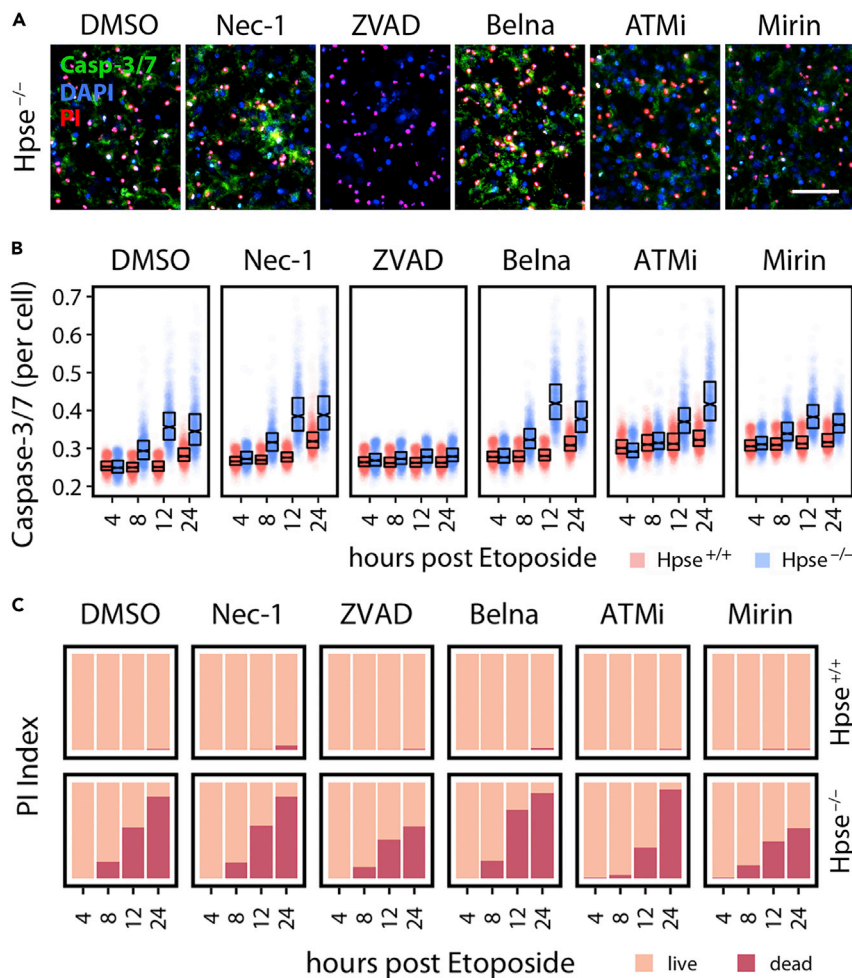


Figure 5. Inhibitor modulation of cell death induced by DNA damage

(A) Representative immunofluorescence micrographs of Hpse^{-/-} MEFs treated with etoposide (50 μM) for 12 h in the presence of specified inhibitors. Scale bar, 100 μm.

(B) Thresholded image intensity quantification analysis of CellEvent caspase-3/7 green detection reagent in Hpse^{+/+} and Hpse^{-/-} MEFs treated with etoposide and specified inhibitors at corresponding times performed with CellProfiler, as introduced in Figure 3. Boxplots indicate medians and interquartile ranges of 250 cells for each of the 4 images for a total of 1,000 cells analyzed per condition. Experiment was replicated two times with similar results.

(C) Propidium iodide uptake quantified as proportions of live and dead cells in Hpse^{+/+} and Hpse^{-/-} MEFs treated with etoposide and specified inhibitors at corresponding times. Nuclei thresholded in CellProfiler with a propidium iodide intensity of greater than 0.2 were considered dead.

expression at MOI of 1 is that with the higher MOI, a substantial number of HPSE-deficient cells are in the process of cell death and the initial exaggerated IFN induction has likely already occurred by the time this qPCR snapshot was collected. Likewise, transcription of the downstream ISG15 is dramatically elevated in HPSE-deficient cells and is unchanged by HSV-1 or etoposide, suggesting that the interferon system is constitutively enhanced in the absence of HPSE.

Here and in prior work, we show that HPSE restricts multiple essential cellular defense responses previously linked to one another but not through one factor: type I interferon, cell death, DNA damage, and regulation of the cell cycle (Agelidis et al., 2021). With these related cellular processes in mind, we looked to the multifunctional transcription factor ATM for its potential involvement in the differential regulation by HPSE. Sensing of DNA damage through p-ATM has been shown to be a potent inducer of interferon production and eventual cell death in numerous studies (Dunphy et al., 2018; Hartlova et al., 2015; Kondo et al., 2013; Yu et al., 2015), yet the precise interactions and kinetics of signaling intermediaries including γH2Ax,

p-CHK2, and the MRN complex remain unclear (Collins et al., 2020). Double-stranded DNA breaks, such as those caused by ionizing radiation or topoisomerase inhibition, result in the activation of serine/threonine kinases ATM and DNA-PK and subsequent phosphorylation of several hundred protein targets, with γ H2Ax serving in many studies as a marker of DNA damage response activation (Jackson and Bartek, 2009; Natale et al., 2017). Likewise, the checkpoint kinase CHK2 is one of the most studied ATM targets, which functions in cell-cycle arrest and control of DNA repair (Shiloh, 2003). Our observation of increased γ H2Ax and p-CHK2 levels in HPSE-deficient cells upon both etoposide and HSV-1 treatment thus suggests an inhibitory role of HPSE in the regulation of DNA damage response. Furthermore, our finding in HPSE-deficient cells that mirin reduces DNA damage-driven apoptosis indicates that HPSE interaction with the MRN complex is likely instrumental in dictating downstream responses and cell fate.

Given the extensive list of interacting proteins identified here by IP-MS and previously by other investigators, HPSE may be capable of this type of regulatory activity in a variety of cellular settings and pathways. Recent work has shown that HPSE binds to DNA with unknown consequences (He et al., 2012; Nobuhisa et al., 2007; Schubert et al., 2004; Yang et al., 2015). Future experiments including nuclease treatment of immunopurified HPSE may show whether any of the associations identified are due to bridging interactions with DNA. Further biochemical analysis of MRN complex binding to ATM in the context of HPSE will clarify the nature of this regulatory system. Interestingly, multiple forms of cancer display increased expression of HPSE, understood to drive late-stage metastatic disease (Purushothaman et al., 2011; Putz et al., 2017; Vlodavsky and Friedmann, 2001; Vlodavsky et al., 2018). These newly observed functions of HPSE can help explain the cell cycle dysregulation and loss of sensitivity to DNA damage observed in malignancy. In parallel, multiple viruses including HSV-1 are known to manipulate DNA damage responses and other cellular stress responses to promote their own replication and spread (Lilley et al., 2005; Luftig, 2014; Moretti and Blander, 2017; Turnell and Grand, 2012). Likewise, HPSE upregulation may provide a survival advantage to dysplastic or infected tissue by enabling cells to avoid detection of insults to DNA common to the processes of microbial infection and tumorigenesis.

Limitations of the study

Although widely used to study the impact of a particular gene, murine embryonic knockout cells present potential limitations, including the possibility of compensatory mechanisms that act to minimize the cellular effect of the genetic defect. It remains to be fully understood whether our findings are the direct result of the presence or absence of HPSE, or related to compensatory alterations that occurred during the knockout process. Our approach from multiple experimental angles including IP-MS of human HPSE and functional analysis of HPSE-deficient MEFs represents an introductory understanding of the role of HPSE and its interactor in the regulation of the DNA damage response. Further demonstration in models such as HPSE complementation of knockout cells and Crispr-Cas9 knockout of human cells will provide additional clarifying details of these findings.

Resource availability

Lead contact

Further information and requests for resources may be addressed to the lead contact, Deepak Shukla, PhD at dshukla@uic.edu.

Materials availability

This study did not generate new unique reagents.

Data and code availability

Raw data for IP-MS proteomics experiment can be found on ProteomeXchange under the identifier PXD014183.

METHODS

All methods can be found in the accompanying [Transparent methods supplemental file](#).

SUPPLEMENTAL INFORMATION

Supplemental Information can be found online at <https://doi.org/10.1016/j.isci.2021.102242>.

ACKNOWLEDGMENTS

This work was supported by NIH grant R01EY029426 (DS), NIH fellowship F30EY025981 (AA), and departmental core grant P30EY001792 (DS).

AUTHOR CONTRIBUTIONS

Conceptualization, A.A. and D.S.; Methodology, A.A., R.K.S., C.D.P., A.C., D.J.G., and D.S.; Software, A.A., A.C.; Validation, A.A., R.K.S., C.D.P., and A.C.; Formal analysis, A.A. and A.C.; Investigation, A.A., R.K.S., C.D.P., and A.C.; Resources, A.A., A.C., D.J.G., and D.S.; Data curation, A.A. and A.C.; Writing – original draft, A.A.; Writing – review and editing, A.A., R.K.S., C.D.P., A.C., D.J.G., and D.S.; Visualization, A.A.; Supervision, A.A., D.J.G. and D.S.; Funding acquisition, A.A. and D.S.

DECLARATION OF INTERESTS

The authors declare no competing interests.

Received: September 30, 2020

Revised: February 9, 2021

Accepted: February 24, 2021

Published: March 19, 2021

REFERENCES

- Agelidis, A., and Shukla, D. (2020). Heparanase, heparan sulfate and viral infection. *Adv. Exp. Med. Biol.* 1221, 759–770.
- Agelidis, A.M., Hadigal, S.R., Jaishankar, D., and Shukla, D. (2017). Viral activation of heparanase drives pathogenesis of herpes simplex virus-1. *Cell Rep.* 20, 439–450.
- Agelidis, A., Turturice, B.A., Suryawanshi, R.K., Yadavalli, T., Jaishankar, D., Ames, J., Hopkins, J., Koujah, L., Patil, C.D., Hadigal, S.R., et al. (2021). Disruption of innate defense responses by endoglycosidase HPSE promotes cell survival. *JCI Insight*. In press. <https://doi.org/10.1172/jci.insight.144255>.
- Aquino, R.S., Lee, E.S., and Park, P.W. (2010). Diverse functions of glycosaminoglycans in infectious diseases. *Prog. Mol. Biol. Transl. Sci.* 93, 373–394.
- Belshe, R.B., Leone, P.A., Bernstein, D.I., Wald, A., Levin, M.J., Stapleton, J.T., Gorfinkel, I., Morrow, R.L., Ewell, M.G., Stokes-Riner, A., et al. (2012). Efficacy results of a trial of a herpes simplex vaccine. *N. Engl. J. Med.* 366, 34–43.
- Bommareddy, P.K., Shettigar, M., and Kaufman, H.L. (2018). Integrating oncolytic viruses in combination cancer immunotherapy. *Nat. Rev. Immunol.* 18, 498–513.
- Brameier, M., Krings, A., and MacCallum, R.M. (2007). NucPred—predicting nuclear localization of proteins. *Bioinformatics* 23, 1159–1160.
- Chan, Y.K., and Gack, M.U. (2016). Viral evasion of intracellular DNA and RNA sensing. *Nat. Rev. Microbiol.* 14, 360–373.
- Christensen, M.H., and Paludan, S.R. (2017). Viral evasion of DNA-stimulated innate immune responses. *Cell Mol. Immunol.* 14, 4–13.
- Collins, P.L., Purman, C., Porter, S.I., Nganga, V., Saini, A., Hayer, K.E., Gurewitz, G.L., Sleckman, B.P., Bednarski, J.J., Bassing, C.H., et al. (2020). DNA double-strand breaks induce H2Ax phosphorylation domains in a contact-dependent manner. *Nat. Commun.* 11, 3158.
- Coombe, D.R., and Gandhi, N.S. (2019). Heparanase: a challenging cancer drug target. *Front. Oncol.* 9, 1316.
- Dunphy, G., Flannery, S.M., Almine, J.F., Connolly, D.J., Paulus, C., Jonsson, K.L., Jakobsen, M.R., Nevels, M.M., Bowie, A.G., and Unterholzner, L. (2018). Non-canonical activation of the DNA sensing adaptor STING by ATM and IFI16 mediates NF-kappaB signaling after nuclear DNA damage. *Mol. Cell* 71, 745–760 e745.
- Guo, C., Zhu, Z., Guo, Y., Wang, X., Yu, P., Xiao, S., Chen, Y., Cao, Y., and Liu, X. (2017). Heparanase upregulation contributes to porcine reproductive and respiratory syndrome virus release. *J. Virol.* 91, e00625–17.
- Hadigal, S.R., Agelidis, A.M., Karasneh, G.A., Antoine, T.E., Yakoub, A.M., Ramani, V.C., Djalilian, A.R., Sanderson, R.D., and Shukla, D. (2015). Heparanase is a host enzyme required for herpes simplex virus-1 release from cells. *Nat. Commun.* 6, 6985.
- Hartlova, A., Ertmann, S.F., Raffi, F.A., Schmalz, A.M., Resch, U., Anugula, S., Lienenklaus, S., Nilsson, L.M., Kroger, A., Nilsson, J.A., et al. (2015). DNA damage primes the type I interferon system via the cytosolic DNA sensor STING to promote anti-microbial innate immunity. *Immunity* 42, 332–343.
- He, Y.Q., Sutcliffe, E.L., Bunting, K.L., Li, J., Goodall, K.J., Poon, I.K., Hulett, M.D., Freeman, C., Zafar, A., McInnes, R.L., et al. (2012). The endoglycosidase heparanase enters the nucleus of T lymphocytes and modulates H3 methylation at actively transcribed genes via the interplay with key chromatin modifying enzymes. *Transcription* 3, 130–145.
- Hong, X., Nelson, K., Lemke, N., and Kalkanis, S.N. (2012). Heparanase expression is associated with histone modifications in glioblastoma. *Int. J. Oncol.* 40, 494–500.
- Ivashkiv, L.B., and Donlin, L.T. (2014). Regulation of type I interferon responses. *Nat. Rev. Immunol.* 14, 36–49.
- Jackson, S.P., and Bartek, J. (2009). The DNA-damage response in human biology and disease. *Nature* 461, 1071–1078.
- Jayatilleke, K.M., and Hulett, M.D. (2020). Heparanase and the hallmarks of cancer. *J. Transl. Med.* 18, 453.
- Kondo, T., Kobayashi, J., Saitoh, T., Maruyama, K., Ishii, K.J., Barber, G.N., Komatsu, K., Akira, S., and Kawai, T. (2013). DNA damage sensor MRE11 recognizes cytosolic double-stranded DNA and induces type I interferon by regulating STING trafficking. *Proc. Natl. Acad. Sci. U S A* 110, 2969–2974.
- Kundu, S., Xiong, A., Spyrou, A., Wicher, G., Marinescu, V.D., Edqvist, P.D., Zhang, L., Essand, M., Dimberg, A., Smits, A., et al. (2016). Heparanase promotes glioma progression and is inversely correlated with patient survival. *Mol. Cancer Res.* 14, 1243–1253.
- Lilley, C.E., Carson, C.T., Muotri, A.R., Gage, F.H., and Weitzman, M.D. (2005). DNA repair proteins affect the lifecycle of herpes simplex virus 1. *Proc. Natl. Acad. Sci. U S A* 102, 5844–5849.
- Luftig, M.A. (2014). Viruses and the DNA damage response: activation and antagonism. *Annu. Rev. Virol.* 1, 605–625.
- Mayr, B., and Montminy, M. (2001). Transcriptional regulation by the phosphorylation-dependent factor CREB. *Nat. Rev. Mol. Cell Biol.* 2, 599–609.
- Moretti, J., and Blander, J.M. (2017). Cell-autonomous stress responses in innate immunity. *J. Leukoc. Biol.* 101, 77–86.

- Natale, F., Rapp, A., Yu, W., Maiser, A., Harz, H., Scholl, A., Grulich, S., Anton, T., Hörl, D., Chen, W., et al. (2017). Identification of the elementary structural units of the DNA damage response. *Nat. Commun.* **8**, 15760.
- Nobuhisa, T., Naomoto, Y., Okawa, T., Takaoka, M., Gunduz, M., Motoki, T., Nagatsuka, H., Tsujigiwa, H., Shirakawa, Y., Yamatsuji, T., et al. (2007). Translocation of heparanase into nucleus results in cell differentiation. *Cancer Sci.* **98**, 535–540.
- Orzalli, M.H., and Knipe, D.M. (2014). Cellular sensing of viral DNA and viral evasion mechanisms. *Annu. Rev. Microbiol.* **68**, 477–492.
- Puerta-Guardo, H., Glasner, D.R., and Harris, E. (2016). Dengue virus NS1 disrupts the endothelial glycocalyx, leading to hyperpermeability. *PLoS Pathog.* **12**, e1005738.
- Purushothaman, A., Hurst, D.R., Pisano, C., Mizumoto, S., Sugahara, K., and Sanderson, R.D. (2011). Heparanase-mediated loss of nuclear syndecan-1 enhances histone acetyltransferase (HAT) activity to promote expression of genes that drive an aggressive tumor phenotype. *J. Biol. Chem.* **286**, 30377–30383.
- Putz, E.M., Mayfosh, A.J., Kos, K., Barkauskas, D.S., Nakamura, K., Town, L., Goodall, K.J., Yee, D.Y., Poon, I.K., Baschuk, N., et al. (2017). NK cell heparanase controls tumor invasion and immune surveillance. *J. Clin. Invest.* **127**, 2777–2788.
- Rabelink, T.J., van den Berg, B.M., Garsen, M., Wang, G., Elkin, M., and van der Vlag, J. (2017). Heparanase: roles in cell survival, extracellular matrix remodelling and the development of kidney disease. *Nat. Rev. Nephrol.* **13**, 201–212.
- Rivara, S., Milazzo, F.M., and Giannini, G. (2016). Heparanase: a rainbow pharmacological target associated to multiple pathologies including rare diseases. *Future Med. Chem.* **8**, 647–680.
- Roider, H.G., Manke, T., O’Keeffe, S., Vingron, M., and Haas, S.A. (2009). PASTAA: identifying transcription factors associated with sets of co-regulated genes. *Bioinformatics* **25**, 435–442.
- Schubert, S.Y., Ilan, N., Shushy, M., Ben-Izhak, O., Vlodavsky, I., and Goldshmidt, O. (2004). Human heparanase nuclear localization and enzymatic activity. *Lab Invest.* **84**, 535–544.
- Shiloh, Y. (2003). ATM and related protein kinases: safeguarding genome integrity. *Nat. Rev. Cancer* **3**, 155–168.
- Stanberry, L.R., Spruance, S.L., Cunningham, A.L., Bernstein, D.I., Mindel, A., Sacks, S., Tying, S., Aoki, F.Y., Slaoui, M., Denis, M., et al. (2002). Glycoprotein-D-adjuvant vaccine to prevent genital herpes. *N. Engl. J. Med.* **347**, 1652–1661.
- Thakkar, N., Yadavalli, T., Jaishankar, D., and Shukla, D. (2017). Emerging roles of heparanase in viral pathogenesis. *Pathogens* **6**, 43.
- Traven, A., and Heierhorst, J. (2005). SQ/TQ cluster domains: concentrated ATM/ATR kinase phosphorylation site regions in DNA-damage-response proteins. *Bioessays* **27**, 397–407.
- Turnell, A.S., and Grand, R.J. (2012). DNA viruses and the cellular DNA-damage response. *J. Gen. Virol.* **93**, 2076–2097.
- Vlodavsky, I., and Friedmann, Y. (2001). Molecular properties and involvement of heparanase in cancer metastasis and angiogenesis. *J. Clin. Invest.* **108**, 341–347.
- Vlodavsky, I., Gross-Cohen, M., Weissmann, M., Ilan, N., and Sanderson, R.D. (2018). Opposing functions of heparanase-1 and heparanase-2 in cancer progression. *Trends Biochem. Sci.* **43**, 18–31.
- Vlodavsky, I., Ilan, N., and Sanderson, R.D. (2020). Forty years of basic and translational heparanase research. *Adv. Exp. Med. Biol.* **1221**, 3–59.
- Xu, D., and Esko, J.D. (2014). Demystifying heparan sulfate-protein interactions. *Annu. Rev. Biochem.* **83**, 129–157.
- Yang, Y., Gorzelanny, C., Bauer, A.T., Halter, N., Komljenovic, D., Bauerle, T., Borsig, L., Roblek, M., and Schneider, S.W. (2015). Nuclear heparanase-1 activity suppresses melanoma progression via its DNA-binding affinity. *Oncogene* **34**, 5832–5842.
- Yu, Q., Katlinskaya, Y.V., Carbone, C.J., Zhao, B., Katlinski, K.V., Zheng, H., Guha, M., Li, N., Chen, Q., Yang, T., et al. (2015). DNA-damage-induced type I interferon promotes senescence and inhibits stem cell function. *Cell Rep.* **11**, 785–797.
- Zhang, B., Xiao, W., Qiu, H., Zhang, F., Moniz, H.A., Jaworski, A., Condac, E., Gutierrez-Sanchez, G., Heiss, C., Clugston, R.D., et al. (2014). Heparan sulfate deficiency disrupts developmental angiogenesis and causes congenital diaphragmatic hernia. *J. Clin. Invest.* **124**, 209–221.

iScience, Volume 24

Supplemental information

**Dissociation of DNA damage sensing
by endoglycosidase HPSE**

**Alex Agelidis, Rahul K. Suryawanshi, Chandrashekhar D. Patil, Anaamika
Campeau, David J. Gonzalez, and Deepak Shukla**

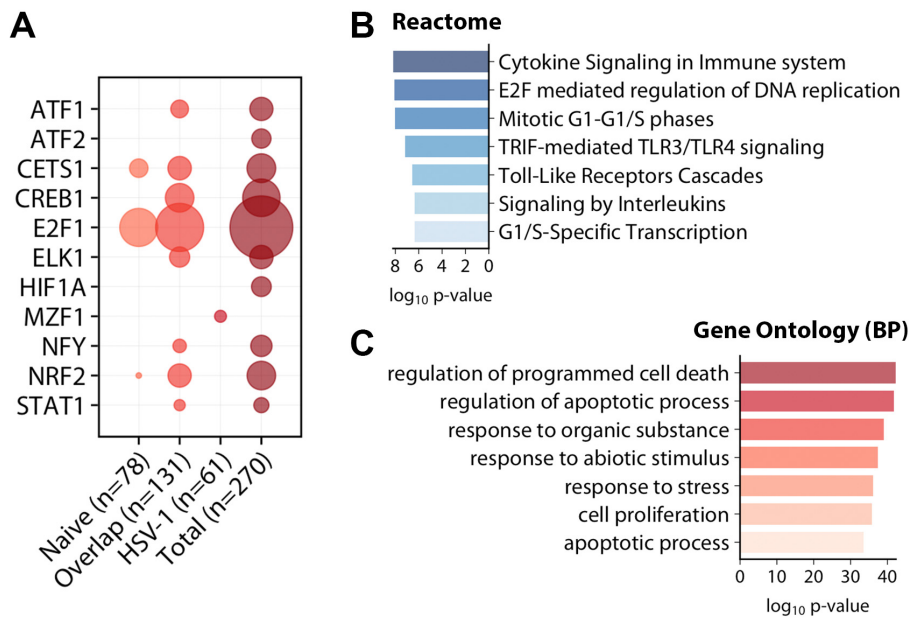


Figure S2 | Transcription factor binding site analysis and extended ontology analysis of immunopurified myc-HPSE proteins links HPSE interactome to regulation of cell cycle, proliferation and cellular responses to stress. Related to Figures 1-2.

(A) Transcription factor binding site enrichment of genes identified in IP-MS analysis performed with PASTAA algorithm default parameters, individually analyzed by Venn diagram segment described in Fig. 1B.

(B-C) Major Reactome (B) and Gene Ontology (C) enrichments of HPSE-binding proteins with newly identified regulatory transcription factors included in the analysis.

Transparent Methods

Key Resources Table

REAGENT or RESOURCE	SOURCE	IDENTIFIER
Antibodies		
XRCC5	Cell Signaling Technology	2180
XRCC6	Cell Signaling Technology	4588
RAD50	Cell Signaling Technology	3427
NBS1	Cell Signaling Technology	14956
myc-Tag	Cell Signaling Technology	2276
phospho-(Ser/Thr) ATM/ATR substrate	Cell Signaling Technology	2851
phospho-(Ser1981) ATM	Cell Signaling Technology	4526
phospho-(Thr68) Chk2	Cell Signaling Technology	2661
phospho-(Ser139) γ H2Ax	Cell Signaling Technology	9718
caspase-8	Cell Signaling Technology	4927
cleaved caspase-8	Cell Signaling Technology	8592
caspase-3	Cell Signaling Technology	14220
cleaved caspase-3	Cell Signaling Technology	9664
caspase-1	Cell Signaling Technology	24232
cleaved caspase-1	Cell Signaling Technology	89332
gasdermin D	Cell Signaling Technology	39754
cleaved gasdermin D	Cell Signaling Technology	10137
isotype control mouse IgG1	Cell Signaling Technology	5415
MRE11	Santa Cruz Biotechnology	sc-135992
GAPDH	Proteintech	10494
Peroxidase AffiniPure goat anti-mouse IgG (H+L)	Jackson ImmunoResearch	115-035-146
Peroxidase AffiniPure goat anti-rabbit IgG (H+L)	Jackson ImmunoResearch	111-035-003
Rabbit anti-mouse FITC	Sigma	F9137
Goat anti-rabbit Alexa Fluor 647	Thermo Scientific	A21244
Bacterial and Virus Strains		
HSV-1 (KOS-WT)	Desai & Person, 1998	N/A
Chemicals, Peptides, and Recombinant Proteins		
KU-55933	Selleckchem	S1092
Necrostatin-1 (Nec-1)	Selleckchem	S8037
ZVAD-fmk	Selleckchem	S7023
Belnacasan	Selleckchem	S2228
Mirin	Selleckchem	S8096
Etoposide	Sigma	E1383
Propidium iodide	Sigma	P4864
NucBlue Live ReadyProbes Hoechst stain	Thermo Scientific	R37605
CellEvent Caspase-3/7 Green Detection Reagent	Thermo Scientific	C10423
Lipofectamine-2000 transfection reagent	Thermo Scientific	11668019

Critical Commercial Assays		
Protein A/G Dynabeads	Thermo Scientific	88802
Trizol	Thermo Scientific	15596018
TMT10plex Isobaric Label Reagent Set	Thermo Scientific	90309
RNeasy Mini kit	Qiagen	74104
Deposited Data		
IP-MS proteomics raw data	ProteomeXchange	PXD014183
Experimental Models: Cell Lines		
Human corneal epithelial cell line	Dr. Kozaburo Hayashi, National Eye Institute	RCB1834 HCE-T
African green monkey: Vero cell line	Dr. Patricia G. Spear, Northwestern University	N/A
Wildtype and Hpse-KO mouse embryonic fibroblasts	Zcharia et al., 2009	N/A
Oligonucleotides		
DNA primers used for qPCR analysis (see section "Quantitative polymerase chain reaction")	Integrated DNA Technologies	N/A
Recombinant DNA		
Myc-GS3 HPSE plasmid	Fux et al., 2009	N/A
Software and Algorithms		
FlowJo v10.0.7	Treestar	N/A
Accuri C6 Plus software	BD Biosciences	N/A
Proteome Discoverer 2.1	Thermo Scientific	N/A
ClueGO v2.5.2 within Cytoscape v3.6.1	Bindea et al., 2009	N/A
CellProfiler	McQuin et al., 2018	N/A
NucPred	Brameier et al., 2007	N/A
PASTAA	Roider et al., 2009	N/A
ZEN	Zeiss	N/A

Experimental Model and Subject Details

Cell lines and virus strains

Human corneal epithelial (HCE) cell line (RCB1834 HCE-T) was obtained from Kozaburo Hayashi (National Eye Institute, Bethesda, MD) and was cultured in MEM (Life Technologies, Carlsbad, CA) with 10% fetal bovine serum (FBS) (Life Technologies) and 1% penicillin/streptomycin (Life Technologies). Confirmation of identity of HCE cell line was done by short tandem repeat analysis. Vero cell line for virus preparation and plaque assay was provided by Dr. Patricia G. Spear (Northwestern University, Chicago, IL) and cultured in DMEM (Life Technologies) with 10% FBS and 1% penicillin/streptomycin. Wildtype and heparanase-knockout mouse embryonic fibroblasts (WT and Hpse-KO MEFs) were provided by Dr. Israel Vlodaysky (Rappaport Institute, Haifa, Israel) (Zcharia et al., 2009). All cells were maintained in a Heracell VIOS 160i CO2 incubator (Thermo Scientific) and have been confirmed negative for mycoplasma contamination. HSV-1 virus used in these studies was KOS-WT strain (Desai and Person, 1998), provided by Dr. Patricia G. Spear (Northwestern University, Chicago, IL). All virus stocks were propagated in Vero cells and stored at -80°C.

Method Details

Antibodies, plasmids and chemical reagents

The following antibodies were used for western blot studies: from Cell Signaling Technology, at dilution 1:1000 – XRCC5 (2180), XRCC6 (4588), RAD50 (3427), NBS1 (14956), myc-Tag (2276) phospho-(Ser1981) ATM (4526), phospho-(Thr68) Chk2 (2661), phospho-(Ser/Thr) ATM/ATR substrate (2851), phospho-(Ser139) γ H2Ax (9718), caspase-8 (4927), cleaved caspase-8 (8592), caspase-3 (14220), cleaved caspase-3 (9664), caspase-1 (24232), cleaved caspase-1 (89332), gasdermin D (39754), cleaved gasdermin D (10137); from Santa Cruz Biotechnology, at dilution 1:250 – MRE11 (sc-135992); from Proteintech, at dilution 1:1000 - GAPDH (10494). The following antibodies were used for immunofluorescence microscopy studies: from Cell Signaling Technology, at dilution 1:100 – phospho-(Ser/Thr) ATM/ATR substrate (2851), phospho-(Ser1981) ATM (4526). HPSE expression constructs including Myc-GS3 plasmid were provided by Dr. Israel Vlodaysky (Rappaport Institute, Haifa, Israel) (Fux et al., 2009). Lipofectamine-2000 transfection reagent (Life Technologies, 11668019) was used for all *in vitro* overexpression experiments, according to the manufacturer's specifications. The following chemical inhibitors were purchased from Selleckchem: KU-55933 (ATMi, S1092) was used to inhibit ATM kinase, Nec-1 (S8037) was used to inhibit necroptosis, ZVAD-fmk (S7023) was used to inhibit apoptosis, belnacasan (S2228) was used to inhibit caspase-1 and mirin (S8096) was used to inhibit the Mre11-Rad50-Nbs1 complex. Etoposide (E1383) was used to induce double stranded DNA breaks and was purchased from Millipore-Sigma.

Western blot

Proteins were extracted from cultured cells using the following lysis buffer: 150 mM NaCl, 50 mM Tris-HCl pH 7.4, 10% glycerol, 1% NP-40, 10 mM sodium fluoride, 1 mM sodium orthovanadate, 10 mM N-ethylmaleimide, and Halt Protease Inhibitor Cocktail (Thermo Scientific). Lysis was performed with periodic vortexing on ice for 30 min, followed by centrifugation at 13,000 rpm for 30 min. Insoluble pellets were discarded and lysates were then denatured at 95°C for 8 min using 4X LDS sample loading buffer (Life Technologies) and 5% beta-mercaptoethanol (Bio-Rad, Hercules, CA). Cellular proteins were separated by SDS-PAGE with NuPAGE 4-12% Bis-Tris 1.5 mm 15-well gels (Thermo Scientific) transferred to nitrocellulose using the iBlot2 system (Thermo Scientific) and membranes were blocked for 1 h in 5% milk/TBS-T, followed by incubation with primary antibody in 5% milk/TBS-T overnight at specified dilutions. Membranes were washed three times in TBS-T and then incubated with species-specific horseradish peroxidase-conjugated secondary antibodies (Jackson ImmunoResearch Peroxidase AffiniPure goat anti-mouse IgG (H+L), 115-035-146 at 1:10,000 or Peroxidase AffiniPure goat anti-rabbit IgG (H+L), 111-035-003 at 1:20,000) for 1 h at room temperature, and upon addition of SuperSignal West Femto substrate (Thermo Scientific), protein bands were detected with Image-Quant LAS 4000 biomolecular imager (GE Healthcare Life Sciences, Pittsburgh, PA).

Quantitative polymerase chain reaction

TRIzol (Thermo Scientific, 15596018) was used to extract total RNA from cultured cells, according to the manufacturer's instructions. Complementary DNA was then produced using High Capacity cDNA Reverse Transcription kit (Thermo Scientific, 4368814). Real-time quantitative polymerase chain reaction (qPCR) was performed with Fast SYBR Green Master Mix (Life Technologies) on QuantStudio 7 Flex system (Life Technologies).

The following mouse-specific primers were used in this study:

IFN- β Fwd 5'-TGTCCTCAACTGCTCTCCAC-3', Rev 5'-CATCCAGGCGTAGCTGTTGT-3'

ISG15 Fwd 5'-AGCAATGGCCTGGGACCTAAAG-3', Rev 5'-CCGGCACACCAATCTTCTGG-3'

β -actin Fwd 5'-GACGGCCAGGTCATCACTATTG-3', Rev 5'-AGGAAGGCTGGAAAAGAGCC-3'

Confocal immunofluorescence microscopy

Wildtype and Hpse-KO MEFs were cultured in 8-well μ -slides (iBidi, Madison, WI). Cells were fixed in 4% paraformaldehyde for 10 min and permeabilized with 0.1% Triton-X for 10 min at room temperature for intracellular labeling, followed by incubation with primary antibody for 1 h at room temperature. When a secondary antibody was needed, cells were incubated with respective FITC- or Alexa Fluor 647-conjugated secondary antibody (Sigma-Aldrich F9137 or Thermo Scientific A21244) at a dilution of 1:100 for 1 h at room temperature. NucBlue Live ReadyProbes Hoechst stain (Thermo Scientific R37605) was included with secondary antibody stains when applicable, according to manufacturer's specifications. Samples were examined under LSM 710 confocal microscope (Zeiss) using a 63X oil immersion objective. Fluorescence intensity of images was calculated using ZEN software. Where appropriate, image analysis including thresholding of nuclei and cell borders, and fluorescence intensity measurement was performed with CellProfiler (McQuin et al., 2018).

Propidium iodide cell death assay

Wildtype and Hpse-KO MEF were incubated in complete culture medium containing 2 μ g/mL propidium iodide (Sigma P4864) and NucBlue Live ReadyProbes Hoechst stain (Thermo Scientific, R37605) to visualize and quantify permeabilized and total cells, respectively. At specified timepoints post treatment, fluorescence micrographs of RFP, DAPI and brightfield channels were acquired using Biotek Lionheart FX system and image analysis and quantification was performed using Gen5 software.

Flow cytometry

For flow cytometric quantification of cell death by PI uptake, cells were pre-treated with KU-55933 (ATMi) or DMSO vehicle for 18 h, then either infected with HSV-1 KOS (MOI=0.1) for 24 h or incubated with etoposide for 8 h (50 μ M), in medium containing PI and the previously used pre-treatment. At the termination of cellular incubations, cells were collected on ice, washed twice with FACS buffer and analyzed with Accuri C6 Plus flow cytometer (BD Biosciences). BD Accuri C6 Plus software and Treestar FlowJo v10.0.7 were used for all flow cytometry data analysis.

Immunopurification

Immunopurification (IP) of proteins was performed using HCE cells cultured in 15 cm dishes. Cells were collected after specified times of infection and/or treatment, washed with PBS, scraped in cold PBS on ice and transferred to conical tubes. Cells were centrifuged at 1200 rpm for 5 min, then cellular proteins were extracted with lysis buffer: 150 mM NaCl, 50 mM Tris-HCl pH 7.4, 10% glycerol, 1% NP-40, 10 mM sodium fluoride, 1 mM sodium orthovanadate, 10 mM N-ethylmaleimide, and Halt Protease Inhibitor Cocktail (Thermo Scientific). After 30 min of lysis with agitation at 4°C, lysates were centrifuged at 13,000 rpm for 30 min to pellet insoluble cellular debris. IP antibody, myc-Tag (Cell Signaling, 2276), or isotype control (mouse IgG1, Cell

Signaling 5415) were then added to clarified lysates and rotated for 16 h at 4°C. Protein A/G Dynabeads (Thermo Scientific, 88802) were added and samples were rotated for 1 h at 4°C. Four washes with magnetic separation were performed with lysis buffer. Beads were finally resuspended in LDS buffer with 5% beta-mercaptoethanol, denatured at 95°C for 8 min, and SDS-PAGE was performed. For IP-MS experiment, pelleted beads were flash frozen in a slurry of dry ice and 70% ethanol and stored at -80°C until further processing.

Mass Spectrometry-Based Proteomic Sample Preparation and Analysis

Proteomic samples were processed as previously described with minor alterations (Agelidis et al., 2021; Lapek et al., 2017). Briefly, pelleted beads from immunopurification described above were immersed in 8 M urea + 50 mM HEPES pH 8.5 and were subjected to 5 min water bath sonication and 5 min centrifugation at 18,000 x g to separate proteins from magnetic beads. Samples were subjected to disulfide bond reduction in 5 mM DTT, alkylation in 15 mM iodoacetamide and protein precipitation with trichloroacetic acid. Protein isolation and digestion proceeded with LysC endopeptidase (VWR) and trypsin (Promega), followed by desalting with C18 resin columns (Waters) and vacuum drying. Dried peptides were labeled with tandem mass tags (TMT) (Thermo Scientific), resuspended in 30% dry acetonitrile in 200 mM HEPES pH 8.5, multiplexed using bridge channel internal standards, and fractionated on an Ultimate 3000 HPLC with 4.6 mm x 250 mm C18 column. Dried fractions were analyzed on an Orbitrap Fusion with in-line Easy Nano-LC 1000 (Thermo Scientific) and spectral data were analyzed using Proteome Discoverer 2.1. Spectral matching was performed against a *Homo sapiens* reference proteome appended to an HSV-1 reference proteome, and spectra were matched against a target and decoy database generated *in silico* using SEQUEST-HT (Elias and Gygi, 2007). False discovery rate of 1% was used to filter spectra at the peptide and protein level. Data were processed by filtering peptide spectral matches (PSMs) to retain only high quality and low ambiguity spectra, and PSMs were finally summed and normalized against the median bridge channel. Gene ontology analysis was performed with ClueGO v2.5.2 (Bindea et al., 2009) within Cytoscape v3.6.1 and ClusterProfiler v3.10.0 (Yu et al., 2012) in R.

Quantification and Statistical Analysis

Statistical tests including Mann-Whitney and Wilcoxon signed-rank tests were implemented in GraphPad Prism and R where appropriate, as indicated in the figure legends. Details of statistical analysis method and information including *n*, mean, and statistical significance values are indicated in the corresponding sections of the main text, figure legends, or Methods. Experiments were replicated three times with similar results and bar plots represent mean ± SEM unless otherwise specified. A p value of < 0.05 was considered to be statistically significant. *p<0.05, **p<0.01, ***p<0.001, ****p<0.0001; ns, not significant.

Supplemental References

Bindea, G., Mlecnik, B., Hackl, H., Charoentong, P., Tosolini, M., Kirilovsky, A., Fridman, W.H., Pages, F., Trajanoski, Z., and Galon, J. (2009). ClueGO: a Cytoscape plug-in to decipher functionally grouped gene ontology and pathway annotation networks. *Bioinformatics* 25, 1091-1093.

Desai, P., and Person, S. (1998). Incorporation of the green fluorescent protein into the herpes simplex virus type 1 capsid. *J Virol* 72, 7563-7568.

Elias, J.E., and Gygi, S.P. (2007). Target-decoy search strategy for increased confidence in large-scale protein identifications by mass spectrometry. *Nat Methods* 4, 207-214.

Fux, L., Feibish, N., Cohen-Kaplan, V., Gingis-Velitski, S., Feld, S., Geffen, C., Vlodaysky, I., and Ilan, N. (2009). Structure-function approach identifies a COOH-terminal domain that mediates heparanase signaling. *Cancer Res* 69, 1758-1767.

Lapek, J.D., Jr., Lewinski, M.K., Wozniak, J.M., Guatelli, J., and Gonzalez, D.J. (2017). Quantitative Temporal Viromics of an Inducible HIV-1 Model Yields Insight to Global Host Targets and Phospho-Dynamics Associated with Protein Vpr. *Mol Cell Proteomics* 16, 1447-1461.

McQuin, C., Goodman, A., Chernyshev, V., Kametsky, L., Cimini, B.A., Karhohs, K.W., Doan, M., Ding, L., Rafelski, S.M., Thirstrup, D., *et al.* (2018). CellProfiler 3.0: Next-generation image processing for biology. *PLoS Biol* 16, e2005970.

Yu, G., Wang, L.G., Han, Y., and He, Q.Y. (2012). clusterProfiler: an R package for comparing biological themes among gene clusters. *OMICS* 16, 284-287.

Zcharia, E., Jia, J., Zhang, X., Baraz, L., Lindahl, U., Peretz, T., Vlodaysky, I., and Li, J.P. (2009). Newly generated heparanase knock-out mice unravel co-regulation of heparanase and matrix metalloproteinases. *PLoS One* 4, e5181.